European Cells and Materials Vol.47 2024 (pages 91–108) DOI: 10.22203/eCM.v047a07 ISSN 1473-2262

Original Article

GENE ACTIVATED REINFORCED SCAFFOLDS FOR SOX9 DELIVERY TO ENHANCE REPAIR OF LARGE LOAD BEARING ARTICULAR CARTILAGE DEFECTS

M. Joyce[1,2,3], T. Hodgkinson[1], C. Intini[1,2,3], J.E. Dixon[4,5], D.J. Kelly[1,2,3] and F.J. O'Brien[1,2,3,*]

[1]Tissue Engineering Research Group (TERG), Department of Anatomy and Regenerative Medicine, Royal College of Surgeons in Ireland (RCSI), D02 YN77 Dublin, Ireland

[2]Trinity Centre for Biomedical Engineering (TCBE), Trinity College Dublin, D02 R590 Dublin, Ireland

[3]Advanced Materials and BioEngineering Research (AMBER) Centre, D02 YN77 Dublin, Ireland

[4]Regenerative Medicine & Cellular Therapies Division, The University of Nottingham Biodiscovery Institute (BDI), School of Pharmacy, University of Nottingham, NG7 2RD Nottingham, UK

[5]NIHR Nottingham Biomedical Research Centre, University of Nottingham, NG7 2RD Nottingham, UK

Abstract

Articular cartilage (AC) has a poor capacity to repair once damaged, with progressive degeneration often leading to osteoarthritis (OA). While biomaterials fabricated with extra cellular matrix (ECM) native to the AC have shown promise for repair of focal AC defects, several challenges must be overcome for the repair of larger load bearing defects due to poor scaffold mechanical properties and a lack of chondrogenic potential in diseased cells. Here, we develop a method to improve such biomaterials by incorporating a bioabsorbable 3D printed reinforcing framework and the delivery of pro-chondrogenic genes to infiltrating stem cells to enhance chondrogenesis and produce hyaline tissue that is more indicative of healthy AC. A bioabsorbable polycaprolactone (PCL) 3D printed framework was surface treated to improve its hydrophilicity and used to reinforce a collagen hyaluronic acid (CHyA) matrix. The mechanically reinforced scaffolds were then gene-activated (GA) with the chondrogenic transcription factor SOX9 which was complexed with non-viral nanoparticles (NPs) generated using the glycosaminoglycan-binding enhanced transduction (GET) system, before being seeded with human mesenchymal stromal cells (hMSC). After 28 days culture in chondrogenic media, hMSCs on the GA-scaffolds deposited an ECM more indicative of healthy hyaline cartilage compared to the gene free control. SOX9 mRNA expression on the GA scaffold was 2-orders of magnitude higher than on the control, with downstream chondrogenic targets of SOX9 (*COL2α1*, *ACAN*) also expressing significantly higher mRNA levels. Expression of pro-chondrogenic ECM proteins such as COL2, were 17.5 times greater (p = 0.0018) on the GA scaffold which also resulted in enhanced production and spatial distribution of sulphated glycosaminoglycans (sGAG), which are critical to the function of healthy AC. In summary, these findings provide evidence that functionalization of a 3D printed biomimetic pro-chondrogenic scaffold with SOX9 NPs enhances the quality of ECM produced by human stem cells on such mechanically reinforced scaffolds.

Keywords: SOX9, gene activated scaffold, non-viral vector, pro-chondrogenic, bioregenerative, cartilage repair.

***Address for correspondence**: F.J. O'Brien, Royal College of Surgeons in Ireland, Dublin, Ireland. Email: FJObrien@RCSI.com

Introduction

Articular cartilage (AC) has a poor capacity to repair once damaged, with progressive degeneration often leading to osteoarthritis (OA) and the need for a total joint replacement (Hodgkinson *et al*., 2022; Medvedeva *et al*., 2018; Levingstone *et al*., 2016). Globally, over 527 million individuals suffer from OA, making it the most prevalent disability amongst adults in the United States (US), costing the US healthcare system $45 Billion in 2015 (Long *et al*., 2022; Scheuing *et al*., 2023; Li *et al*., 2016; Zhao *et al*., 2019). Concerningly, OA prevalence in younger individuals is expected to increase in the coming decades, caused in part by increasing obesity rates (Leskinen *et al*., 2012). Traditionally, artificial total joint implants have been used as a terminal treatment for OA. However, while successful in the short-term, these implants are costly and prone to loosening and failure over time (Rolfson *et al*., 2009; Deirmengian & Lonner, 2008; Mihalko *et al*., 2020). Tissue engineering and regenerative medicine offers an alternative approach by focusing on promoting cartilage regeneration prior to severe tissue degeneration and loss-of-function (Billings *et al*., 1990; Niemeyer & Angele *et al*., 2022).

Recent advancements in biomaterials for AC defect repair have shown success improving cartilage regeneration in focal AC defects (Levingstone *et al*., 2016; Niemeyer & Angele, 2021). However, biomaterials design for the effective repair of larger AC defects or defects in load bearing regions of cartilage remains a significant challenge as the most successful biomaterials are typically fabricated with extra cellular matrix (ECM) native to the AC. These materials are typically limited in terms of mechanical properties when compared to healthy tissue. Therefore, successful repair strategies must be capable of both withstanding the mechanical loads present in articular cartilage while also promoting and controlling cell-mediated tissue regeneration i.e. retaining biological functionality.

One strategy to address this problem involves the reinforcement of regenerative biomaterials to improve their mechanical properties and more accurately mimic the compressive modulus of healthy AC (0.5-2.0 MPa) (Kabir *et al*., 2021; Schipani *et al*., 2020; Visser *et al*., 2015; Hutmacher *et al*., 2001). Recently, our lab developed a freeze-dried microporous matrix for AC repair with a proven track record of promoting chondrogenic differentiation and improving cartilage defect repair (Intini *et al*., 2022; Levingstone *et al*., 2016), which is comprised of type-I collagen, type-II collagen, and hyaluronic acid (CHyA) that promotes production of type II collagen and sulphated glycosaminoglycans (sGAG) but no significant increase in type X collagen (Levingstone *et al*., 2016; Intini *et al*., 2022; Matsiko *et al*., 2012; Intini *et al*., 2022). To adapt this technology for large defect repair, this CHyA matrix was recently mechanically reinforced, through integration of a 3D printed bioabsorbable lattice comprised of polycaprolactone (PCL) (Joyce *et al*., 2023). This reinforcement increased the compressive modulus of the CHyA scaffold to within the range of native cartilage, while also serving as a secure attachment point to the subchondral bone to ensure adequate cellular and tissue integration when paired with a microfracture surgical technique (Joyce *et al*., 2023). This approach can feasibly shield biomaterial-resident cells from excessive compressive forces during loading and reduce mechanically-driven increases in inflammation and catabolic enzyme production (Hodgkinson *et al*., 2022; Selig *et al*., 2020). Importantly, this approach allows integration of this mechanical reinforcement with softer, regenerative biomaterials that support chondrogenic differentiation and production of articular cartilage-like ECM (Joyce *et al*., 2023; Lotz *et al*., 2021; Sheehy *et al*., 2019). Initial studies have demonstrated that this reinforcing structure can be designed to have a positive impact on chondrogenesis, even in static culture conditions, significantly increasing sulphated glycosaminoglycans (sGAG) deposition (Critchley *et al*., 2020). However, it is expected that effective treatment of larger area AC defects will require additional stimulation to ensure adequate hyaline tissue formation and to ensure invading cells adopt the correct phenotype.

To promote AC repair, recombinant growth factors (rGFs) have been typically used to enhance the regenerative potential of biomaterials (Chen *et al*., 2020; Holland *et al*., 2005). Unfortunately, the short molecular half-life of rGFs makes delivering an effective and sustained localized dose *in vivo* difficult. This means that often supraphysiological doses or repeated delivery of rGFs are required, which can limit spatial control and increasing the risk of off-target effects, adverse outcomes and costs (Qi *et al*., 2019; Lee *et al*., 2011). By contrast, delivery of pro-chondrogenic gene therapies on chondro-supportive biomaterials have been shown to locally deliver effective and sustained doses, with positive physiological benefits being observed *in vitro* and *in vivo* when treating focal AC defects (Raftery *et al*., 2019; Venkatesan *et al*., 2018; Venkatesan *et al*., 2022; Carballo-Pedrares *et al*., 2022; Raftery *et al*., 2020). These gene therapies are typically delivered using viral vectors, although our lab has put particular focus on non-viral scaffold-based gene delivery for indications including bone, nerve, skin as well as cartilage (Raftery *et al*., 2019; Walsh *et al*., 2021; Laiva *et al*., 2021; Walsh *et al*., 2019; Laiva *et al*., 2021). The aim of this study was to gene activate our previously developed mechanically reinforced biomaterial (PCL-CHyA) (Joyce *et al*., 2023) with a proven history of supporting chondrogenesis to further enhance production of hyaline-like ECM for the treatment of large area AC defects including in tissues suffering from compromised biological functionality.

Our focus with this gene activated scaffold platform is ultimately to target resident stem cells in the bone marrow beneath the surface of the articular joint. The surgical procedure of microfracture is used commonly clinically to release human mesenchymal stromal cells (hMSC) from the bone marrow to attempt to repair AC defects. However, the resultant tissue formed is predominantly inferior fibrocartilage which is rich in type-I collagen whereas the collagen composition in healthy AC tissue is ~ 95 % type-II collagen (Sophia *et al*., 2009; Cohen *et al*., 1998). We thus propose to use gene delivery of pro-chondrogenic factors to enhance the ability of these MSCs to effectively repair large defects. The SRY-box transcription factor 9 (SOX9) was identified and selected as the target gene based on its well understood and documented role as a master chondrogenic transcription regulator (Rey-Rico *et al*., 2018; Jo *et al*., 2014; Haudenschild *et al*., 2010; Lefebvre *et al*., 2019). Therefore, we hypothesized that gene activating the mechanically reinforced pro-chondrogenic PCL-CHyA scaffolds would further enhance chondrogenic differentiation of infiltrating hMSCs, leading to higher quality ECM deposition more indicative of healthy articular cartilage ECM, for the purported treatment of larger AC defects.

The specific objective of this study was thus to complex p*SOX9* with non-viral nanoparticles (NPs) and deliver them on a mechanically reinforced PCL-CHyA scaf-

fold. Gene delivery was mediated by the use of the Glycosaminoglycan-binding enhanced transduction (GET) system which has previously been successfully exploited in a number of applications (Intini *et al*., 2023; Eltaher *et al*., 2022; Power *et al*., 2022; Blokpoel *et al*., 2021; Blokpoel *et al*., 2020; Abu *et al*., 2020; Jalal & Dixon, 2020; Ritchie *et al*., 2020). Validation of the SOX9 activated scaffolds were conducted by assessing their ability to promote the chondrogenic differentiation of hMSCs compared to gene free control scaffolds. Expression of pro-chondrogenic, and hypertrophic genes, along with secreted ECM components were assessed to determine the effect of SOX9 activated scaffolds on chondrogenic differentiation. The developed approach has great potential to be used as an off-the-shelf solution for the treatment of large area AC defects which have very limited treatment options currently available.

Materials and Methods

Biofabrication of Mechanically Reinforced Biomimetic Scaffolds

A collagen and hyaluronic acid (CHyA) slurry was created by blending 0.9g of bovine type I collagen (Collagen Matrix, Paramus, NJ, USA) (0.25 % w/v) and 0.9 g of porcine type II collagen (Symatese, Chaponost, France) (0.25 % w/v) in 300 mL of 0.5 M acetic acid. Then 0.18 g of hyaluronic acid (1.50-1.80 MDa) (Contipro, Dolní Dobrouč, Czech Republic) (0.05 % w/v) was added dropwise as previously described by Matsiko *et al.* (2012). The CHyA slurry was combined with 3D printed PCL scaffolds as described (Joyce *et al*., 2023). Briefly, PCL (Polysciences, Hirschberg an der Bergstrasse, Germany) scaffolds (2 mm height × 10 mm diameter) were 3D printed with an Allevi II (Allevi, Philadelphia, PA, USA) with a continuous non-intersecting gyroid infill pattern. PCL scaffolds were surface treated in 3 M NaOH for 48 hours, to cleave ester bonds on the surface of the PCL making it more hydrophilic, while also micro-etching the surface of the PCL to increase its roughness on the microscopic scale. Surface treated gyroid scaffolds were rinsed three times with diH_2O to remove excess NaOH. PCL scaffolds were placed in a cylindrical steal mold with CHyA slurry being pipetted into the mold to occupy the remaining space, before they were degassed together. The complexed PCL-CHyA then underwent a 48-hour freeze drying cycle to –20 °C as previously described by Matsiko *et al.* (2012), (Joyce *et al*., 2023; Matsiko *et al*., 2015; Haugh *et al*., 2011). After freeze-drying was complete, PCL-CHyA scaffolds were crosslinked for two hours at pH 5.0 with 1-Ethyl-3-(3(dimethlaminopropyl)-carbodimide (EDAC) (Sigma-Aldrich, St. Louis, MO, USA) and N-Hydroxysuccinimide (NHS) (Sigma-Aldrich, St. Louis, MO, USA) in a 5:2 molar ratio (EDAC:NHS) using 70 % EtOH as a solvent. Scaffolds were then rinsed three times with sterile PBS prior to use.

Plasmid DNA Amplification and Isolation in E.coli

The non-integrating plasmid for SOX9 (NM_000346) was supplied by OriGene (*SC321884*, OriGene, Rockville, MD, USA). The plasmid was amplified in chemically competent *E.coli* (ThermoFischer OneShot-C404010, USA), and isolated with an EndoFree Plasmid DNA isolation kit (#12362, Qiagen, Hilden, Germany) following the manufacturer's protocol.

Nanoparticle Complexation and Optimization

SOX9 nanoparticle (NP) complexation was performed as previously described (Raftery *et al*., 2019). In short, 3 different charge ratios (CR: 6, 9, 12) were complexed by varying the relative mass of a cell penetrating peptide (GET) to the mass of the pDNA cargo within OptiMEM (30 µL) (Gibco, Loughborough, UK). We have previously used the GET peptide for gene delivery in a number of indications (Raftery *et al*., 2019; Intini *et al*., 2023; Eltaher *et al*., 2022; Power *et al*., 2022; Markides *et al*., 2019). To compare transfection efficiencies of the SOX9 GET NPs to a commercially available lipid nanoparticle (LNP) vector system, Lipofectamine^{TM} 3000 (L3000015, ThermoFisher Scientific, Carlsbad, CA, USA) was utilized based on its documented use and availability commercially (Khaitov *et al*., 2021; Park *et al*., 2011). Equal amounts of pDNA were delivered with LNP as with GET and complexed according to the manufacturer's protocol (Thermo Fisher Scientific Inc, 2016). pDNA quantity between 2D, and 3D experiments were scaled relative to cell number, with ~ 4 picograms of pDNA delivered per hMSC.

Gene Activation of Reinforced Scaffolds with SOX9 Nanoparticles

Prior to cellular seeding, sterile cylindrical PCL-CHyA scaffolds (2 mm × 10 mm) had 1 µg of pDNA with complexed vectors (GET, LNP) suspended in OptiMEM, pipetted onto the superficial cylindrical face, before the microporous scaffold was flipped and the opposing face had an additional 1 µg of pDNA pipetted onto it, making a total of 2 µg pDNA per gene activated scaffold. The LNP control was pipetted onto the scaffold similar to the SOX9 NPs. However, 4 hours after seeding cells on the LNP scaffolds, a media change was performed with growth media (GM) as previously described by Khaitov *et al.* (2021) to decrease the cytotoxicity of Lipofectamine 3000 (Thermo Fisher Scientific Inc, 2016). Whereas cells seeded on SOX9 activated scaffolds remained in the initial GM for 24 hours before receiving a media change to CCM.

Cell Culture Conditions

Human bone marrow derived mesenchymal stromal cells (hMSC) (Rooster Bio, USA) from 3 donors were expanded to P5 before being seeded on reinforced scaffolds (5 × 10^5 cells/scaffold) as previously described (Joyce *et al*., 2023). hMSCs were expanded in growth media (GM) con-

sisting of low glucose Dulbecco's Modified Eagle Medium (DMEM) with 10 % FBS, and 1 % penicillin/streptomycin. Complete chondrogenic media (CCM) consisting of low glucose DMEM supplemented with TGFβ-3 as previously described (Joyce *et al*., 2023) was used after hMSCs were seeded on reinforced scaffolds.

Maximizing NP Transfection Efficiency for hMSCs on 3D Reinforced Scaffolds

To maximize transfection efficiency of hMSC within the pro-chondrogenic scaffolds, 3 different charge ratios (CR) of 6, 9, and 12 were complexed with a reporter plasmid (p*Gaussia Luciferase)* by varying the mass of GET NPs to pDNA. Media samples were collected at 24, 72, and 168 hours and analyzed with a Luciferase Flash Assay (Thermo Fisher Scientific, Bridgewater, NJ, USA), to determine transfection efficiency non-destructively.

Validation and Spatial Characterization of SOX9 Transgene Expression with Immunocytochemistry

Immunocytochemistry (ICC) was performed to confirm that pSOX9 transfections led to an increase in SOX9 protein and determine if SOX9 was successfully shuttled into the nucleus. Therefore, 7 days after transfection in 2D culture ICC analysis was performed with antibodies specific for SOX9 (1:250, ab182579, Abcam, UK), using a secondary antibody conjugated with Alexa Fluor 568 (1:200, ab175473, UK). Samples were counterstained with DAPI at a 1:500 dilution before being imaged with a Leica DFC520C camera (Leica Microsystems, Wetzlar, Germany) on a microscope (AE31E, Motic, Germany). Confirmation of transfection and spatial localization was performed visually by overlapping images of DAPI nuclear staining with SOX9 antibody expression with ImageJ software version 1.53K (LOCI, University of Wisconsin, Madison, WI, USA). The percentage of transfected cells was calculated by counting SOX9 positive cells relative to total DAPI stained cells.

Analysis of Gene Expression Regulating Chondrogenesis

Relative changes in mRNA expression of hMSC seeded on 3D scaffolds were quantified using qRT-PCR with the $\Delta\Delta$Ct method (Rao *et al*., 2013). After culture, cell seeded PCL-CHyA scaffolds were lysed in QIAzol (Qiagen, Manchester, UK) before having their mRNA extracted using a RNeasy extraction column (Qiagen, Manchester, UK) and a QuantiTect Reverse Transcription (RT) kit (Qiagen, Manchester, UK) to convert the mRNA into cDNA. qRT-PCR was performed and quantified with a QuantiStudio 3 Real Time PCR system (Applied Biosystems, Blanchardstown, Ireland), utilizing SybrGreen (PB20.14-05, PCR-Biosystems, London, UK) in conjunction with Qiagen QuantiTect PCR primers: SRY (sex determining region Y)-box 5 (SOX5) (QT00084784), SRY (sex determining region Y)-box 6 (SOX6) (QT01022539), SRY (sex determining region Y)-box 9 (SOX9) (QT00001498), Type II collagen alpha 1 chain (COL2A1) (QT00049518), Aggrecan (ACAN) (QT00001365), Type X collagen alpha 1 chain (COL10A1) (QT00096348), Runt-related transcription factor 2 (RUNX2) (QT00020517), and Glyceraldehyde 3-phosphate dehydrogenase (GAPDH) (QT00079247). PCR data was normalized against GAPDH expression.

Analysis of Pro-Chondrogenic Protein Expression

Western blot (WB) protein analysis was performed to compare relative protein expression between hMSCs on SOX9 activated scaffolds and their gene free control. For SDS-PAGE, 15 µg of denatured total protein samples from individual biological repeats with 4× Laemmli sample buffer (#1610747, BioRad, Watford, UK) were loaded and ran in Mini-PROTEAN TGX electrophoresis gels (#4561094, BioRad, Watford, UK) at 150 volts for 50 minutes. Proteins within the polyacrylamide gels were then transferred to 0.2 µm PVDF membranes with a Trans-Blot Turbo Transfer Pack (#1704156, BioRad, Watford, UK).

Membranes were blocked (5 % (w/v) powdered milk in tris-buffered saline with 0.1 % tween-20 TBST) and incubated overnight at 4 °C with a primary rabbit antibody specific to human SOX9 (ab182579), or COL2A1 (ab188570). Membranes were washed 3 times with TBST, before membranes were incubated in a secondary antibody (goat anti-rabbit IgG-HRP (ab205718)) for one hour at room temperature. After washing three times in TBST, membranes were treated with 1mL of enhanced chemiluminescence (ECL) substrate (BioRad, Watford, UK) and imaged on a GE Amersham 600 chemiluminescent imager. Membranes were stripped (15 g Glycine, 1 g SDS, 10 mL Tween-20, 1 L diH_2O) at a pH of 2.2, before blocking and incubation with GAPDH (ab9485) antibodies at a 1:5000 dilution. As previously described, membranes were then washed, incubated with HRP conjugated secondary antibodies (goat anti-rabbit IgG-HRP) (ab205718, 1:5000) and imaged in the presence of ECL. Relative protein expression was quantified using ImageJ software to determine signal band intensity relative to the expression of the correlative GAPDH band from each scaffold.

Characterization of cellular health through metabolic activity

An alamarBlue Assay (ThermoFisher Scientific, Eugene, OR, USA) was used as a non-destructive indicator of cellular metabolic viability without terminating the experiment. Cell seeded PCL-CHyA scaffolds were incubated with 10 % AlamarBlue in CCM for 2 hours. Media samples were then measured with a 560 nm/590 nm excitation and emission wavelength respectively to determine relative metabolic activity of cells. Due to the large size, and opaque nature of the 3D microporous PCL-CHyA scaffold, live/dead assays are not an accurate representation of cel-

lular viability, as they are in suspension, or 2D cell culture characterizations (MacCraith *et al*., 2022).

DNA and sGAG Quantification

Sulphated glycosaminoglycans (sGAG) and DNA quantification were both performed by first lysing cell seeded scaffolds with consecutive freeze-thaw cycles prior to digestion with 0.01 % papain (Sigma-Aldrich, Wicklow, Ireland) overnight at 65 °C. A Blyscan sGAG assay (Biocolor, Carrickfergus, UK) (Matsiko *et al*., 2015; Manual, 2012), and a Quant-iT PicoGreen dsDNA assay (Invitrogen, Waltham, MA, USA) (ThermoFisher, 2008) were used following their respective manufacturer protocols. In brief, sGAGs were quantified through binding of Blyscan dye and absorbance measured at a wavelength of 656 nm. sGAG concentration was determined by comparison to a standard curve. Similarly, DNA was quantified by intercalating dsDNA with Picogreen, and measuring the fluorescence at a wavelength of 538 nm. dsDNA concentration was also determined by comparison to a standard curve.

Histological Analysis of ECM Deposition

After 28 days in cell culture, scaffolds were rinsed with PBS and fixed in 4 % paraformaldehyde for histological staining. Scaffolds were dehydrated in an ethanol gradient before soaking in Xylene (#534056, Sigma-Aldrich, Overijse, Belgium) to dissolve the reinforcing PCL structure prior to paraffin wax (8002-74-2, Epredia, Kalamazo, MI, USA) embedding. Scaffolds were serially cross-sectioned (10 µm thick) in the axial plane from the top cylindrical face to the bottom, with a microtome (RM2255, Leica Microsystems, Wetzlar, Germany). Histological sections were deparaffinized and rehydrated through an ethanol gradient before staining with 2 % Alcian Blue (pH = 1) (A5268, Sigma-Aldrich, USA) and a nuclear-red counter stain (#1.00121, Merck, Darmstadt, Germany). After staining, samples were imaged with a Nikon Eclipse 90i microscope (Nikon Co, Tokyo, Japan) and Nikon DS RiL camera (Nikon Co, Tokyo, Japan). Entire cross-sectional slices of scaffolds were consecutively imaged at 10× magnification to create high resolution mosaic images. For transparency, full-layer histological slices are shown at incremental depths, in addition to magnified regions of interest, to give the fairest representation of results.

Additionally, immunohistochemical (IHC) analyses were performed on histological sections to characterize the extracellular matrix deposition spatially. Sections from the upper superficial region (0-500 µm depth) were incubated overnight at 4 °C with a mouse primary antibody for COL2 (SC52658, Santa Cruz, CA, USA) at a 1:100. A secondary antibody specific to mouse IgG conjugated with HRP (ab6728, Abcam, Cambridge, UK) in a 1:500 dilution was incubated for 1 hour. Samples were treated with Avidin Peroxidase in blocking buffer (45 min). Then treated with a DAB substrate peroxidase kit (SK-4100, Vector Laboratories, Newark, CA, USA) for 10 minutes. Sections were mounted with coverslips and imaged with a Nikon DS RiL camera as previously.

Statistical Analysis

3D cell culture experiments were repeated with 3 separate donor populations of hMSCs. Each donor had its own biological repeats (n = 3). Data from the 9 scaffolds from each treatment group were weighted equally, n = 9. Graphical data points are color coded to denote different donor populations (– Donor 1, – Donor 2, –Donor 3). Significant statistical differences between treatment groups were calculated using Prism GraphPad software version 9.3.1 (Prism, San Diego, CA, USA). One-way analysis of variance (ANOVA) with a Tukey post-hoc test for multiple comparisons between all groups, with a 95 % confidence interval (CI) was utilized when appropriate. Alternatively at times as indicated in figure legends, ANOVA with Fisher's LSD test were utilized when appropriate. When comparing only two separate treatments, two tailed *T* tests were performed. All figures have *p* values expressed as: $*p < 0.05$, $**p < 0.01$, $***p < 0.001$, $****p < 0.00001$.

Results

NP Charge Ratio was Optimized for hMSC Transfection in 3D Pro-Chondrogenic Reinforced Scaffolds

To determine the optimal charge ratio of GET NP to pDNA to transfect hMSCs within 3D scaffolds (2 mm × 10 mm), a reporter plasmid (*Gaussia Luciferase*) was complexed with the delivery peptide at three different charge ratios (6, 9, 12) (Fig. 1**a**). No significant difference in luciferase expression was observed between the 3 CR treatment groups and the gene free control at the 24-hour timepoint. However, there was a significant increase in secreted luciferase 3 days after transfection in all three treatment groups compared to the gene free control. Only two of the three treatment groups (CR6, CR9) sustained significant production of luciferase expression 7 days post transfection. Luciferase expression in the CR12 group was not significantly different from the gene free control at D7 ($p = 0.4081$). Since CR9 presented the highest luciferase expression in 2/3 timepoints, this CR was selected for all future transfections on gene activated scaffolds.

Successful SOX9 Upregulation Lead to Increased Nuclear SOX9

Successful transfection of hMSCs with SOX9 NPs in 2D culture was confirmed through ICC at 7 days post-transfection, with a detectable upregulation of the SOX9 protein observed in comparison to gene free controls (Fig. 1**b**). Importantly ICC confirmed with DAPI counterstaining that detectable SOX9 protein was spatially located within the nucleus, which is required for it to perform as a pro-chondrogenic transcriptional regulator. While basal levels were observed in the gene free sample with 6 % of

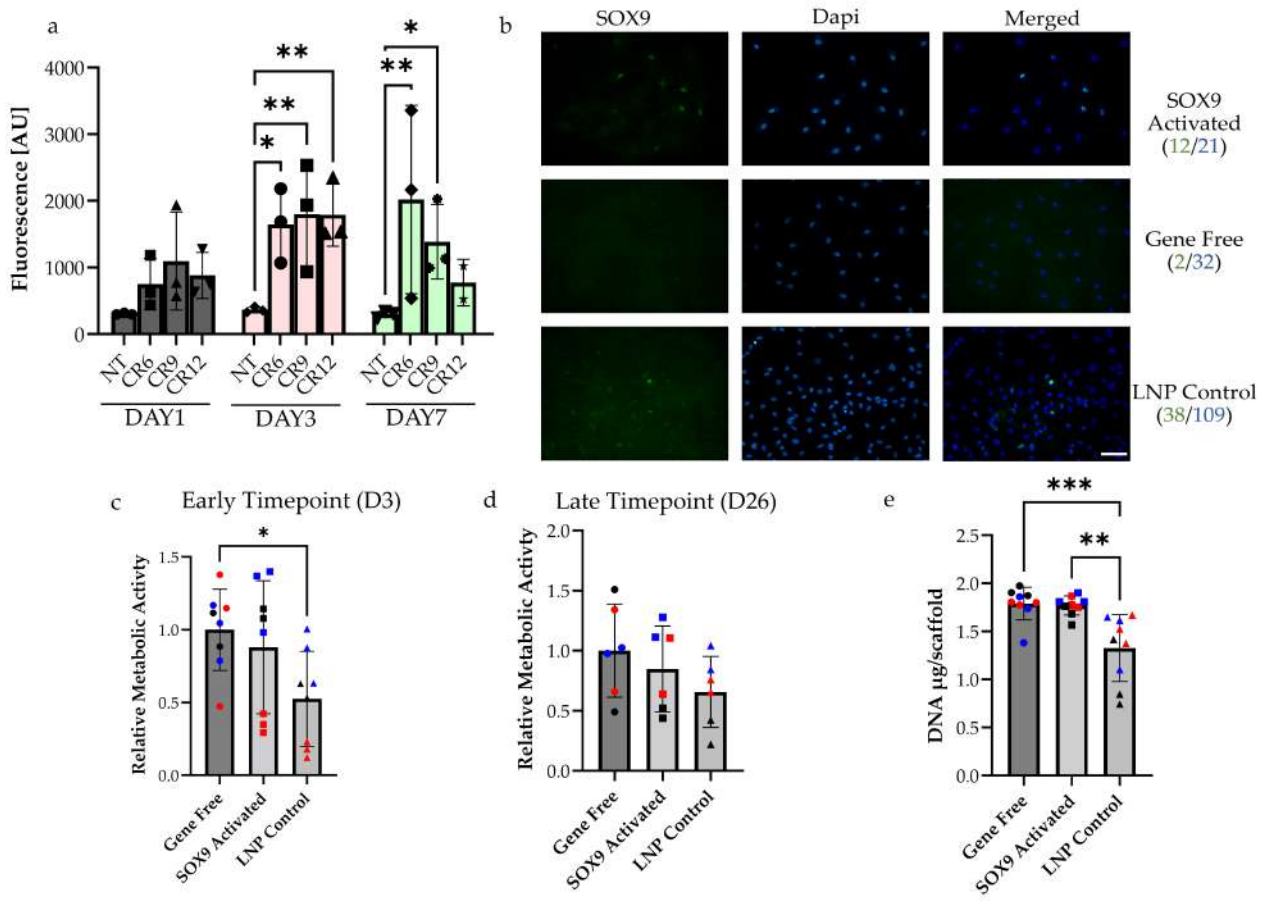

Fig. 1. Successful optimization and validation of hMSC transfection in 2D and within 3D scaffolds. (**a**) Expression of Luciferase from hMSC on gene activated scaffolds at charge ratios 6, 9, and 12 collected after 1, 3, and 7 days in culture. One-way ANOVA with Fisher's LSD test between CR groups and their gene free control determined significance (n = 3, *p < 0.05, **p < 0.01). (**b**) Immunocytochemistry with primary antibodies for SOX9 (ab182579, 1:250 dilution) indicate hMSC transfection in 2D culture with SOX9 NPs lead to increased SOX9 expression (green), localized within the DAPI stained nucleus (blue), as seen in the merged column where transfected cells (green) of total DAPI stained cells (blue) are quantified and expressed as fration under the row title (n = 1 well), scale bar = 200 µm. (**c**) Alamar blue quantified metabolic activity of hMSCs on scaffolds at 3 days (n = 9) and (**d**) 26 days (n = 6) in culture. (**e**) DNA content (µg/scaffold) was quantified at the termination of hMSC scaffold cultures (D28) (n = 9). (*p < 0.05, **p < 0.01, ***p < 0.001) (– Donor 1, – Donor 2, ─Donor 3). hMSC, human mesenchymal stromal cells; ANOVA, analysis of variance; CR, charge ratios; NPs, nanoparticles.

DAPI$^+$ cells expressing detectable levels of SOX9. Expression was enhanced with treatment of SOX9 NPs, and LPN transfection groups with their respective 57 % and 35 % of DAPI$^+$ cells expressing detectable levels of SOX9 expression.

hMSCs on SOX9 Activated Scaffolds Maintain Normal Metabolic Activity and DNA Synthesis

Metabolic activity of hMSCs on reinforced scaffolds were measured as a non-invasive indication of cellular health. There was no significant reduction in metabolic activity in hMSCs cultured on the SOX9 activated scaffold compared to the gene free scaffold control after 3 (Fig. 1**c**), or 26 days (Fig. 1**d**). Conversely, hMSCs cultured on LNP control scaffolds showed a significant reduction in their metabolic activity compared to the control after 3 days (p = 0.0407) (Fig. 1**c**). After 26 days in culture the LNP control group was able to recover slightly with no significant change in metabolic activity from the gene free control (Fig. 1**d**). However, DNA quantification revealed significantly lower levels of DNA present at the experiment end point (Day 28) in LNP scaffold groups than both the gene free and SOX9 NP treatment groups (p = 0.0008, p = 0.0013, respectively). There was no significant difference in quantified DNA between the SOX9 activated and the gene free control (p = 0.9807) (Fig. 1**e**).

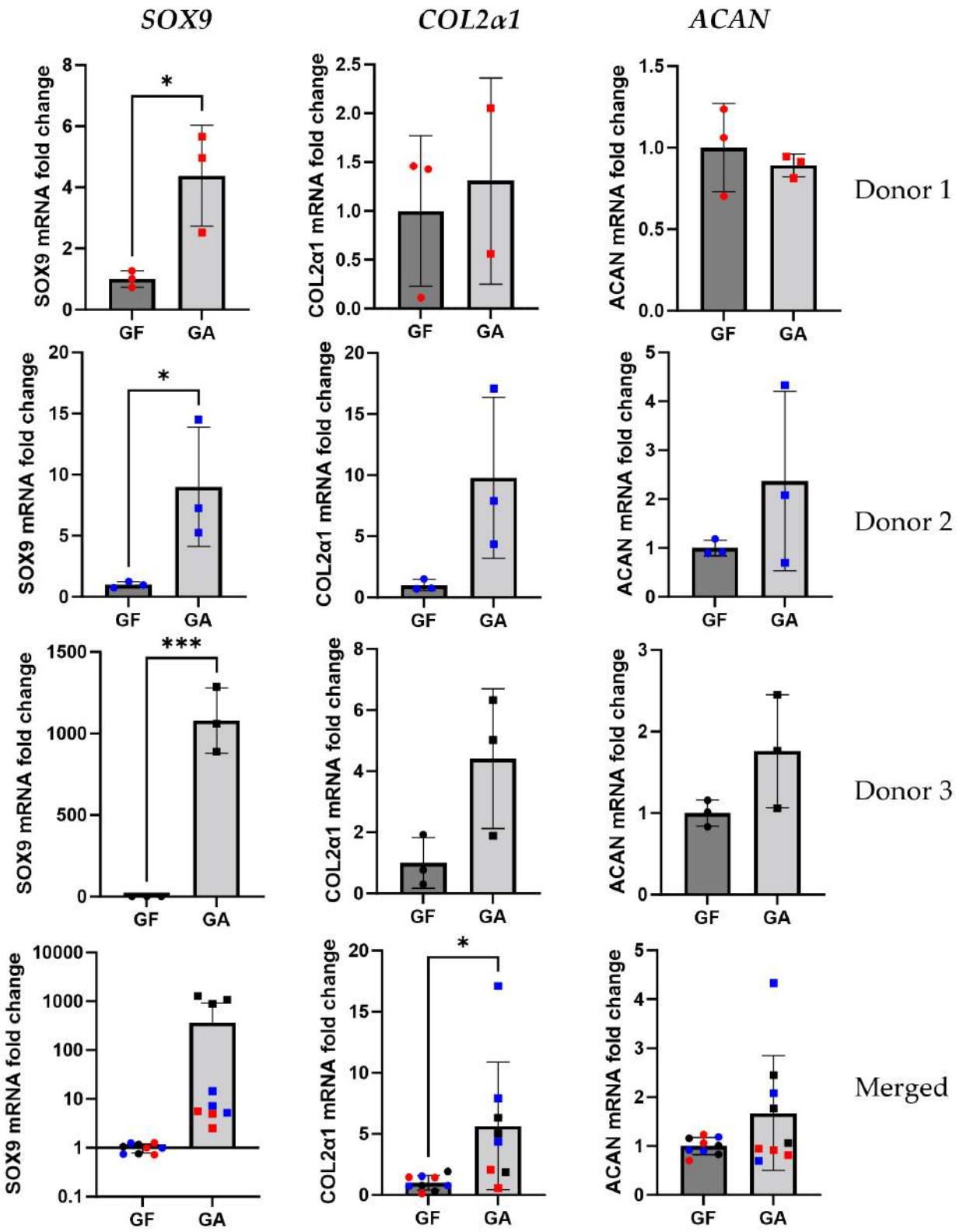

Fig. 2. Gene expression 7 days after transfection confirmed increased SOX9 mRNA expression in hMSCs cultured on SOX9 activated scaffolds. Expression of the *SOX9* transgene, and its downstream targets *COL2α1*, and *ACAN* were analyzed with qRT-PCR from cells on gene free (GF) and SOX9 gene activated (GA) scaffolds. Individual data from 3 donors $n = 3$, and a merger of all donor data sets equally weighted ($n = 9$) are displayed. A two-tailed mean value *T* test determined significance of differences between mean values. (*$p < 0.05$, ***$p < 0.001$) (– Donor 1, – Donor 2, –Donor 3).

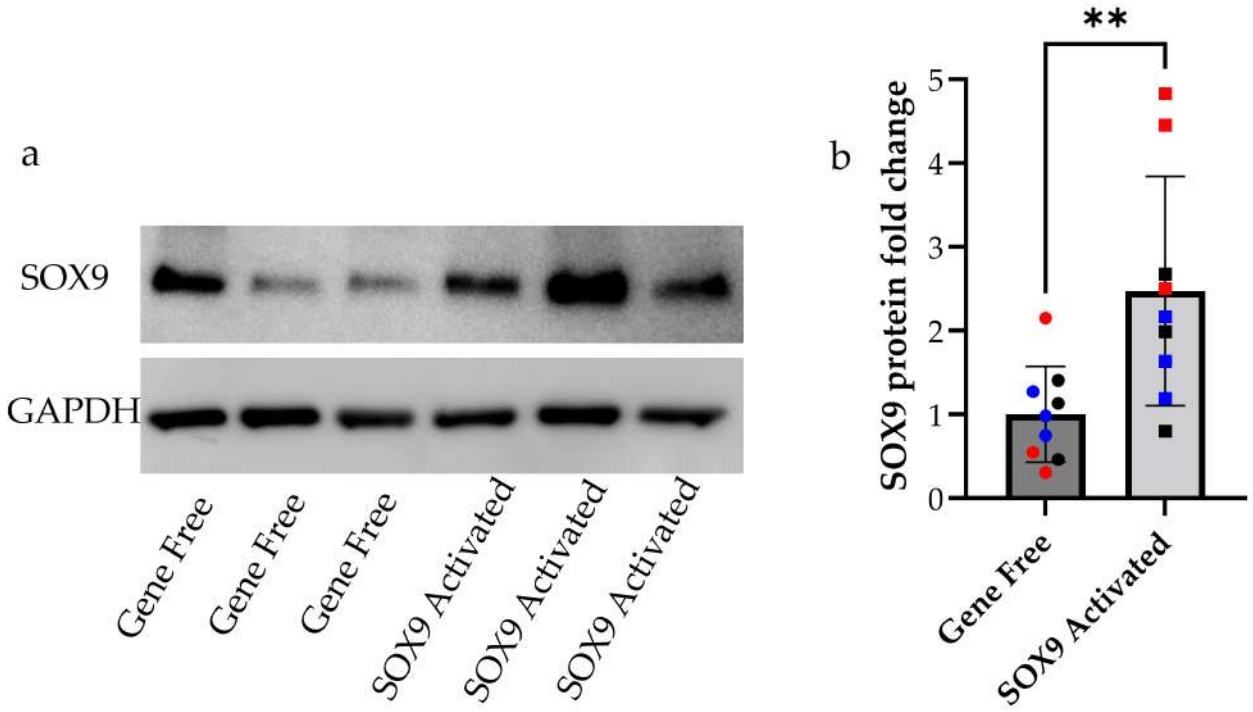

Fig. 3. SOX9 protein expression was upregulated in hMSCs within 7 days of culture on gene activated scaffolds. (**a**) Protein expression (SOX9/GAPDH) comparison between gene free and SOX9 activated scaffolds (n = 3). (**b**) Quantified SOX9 protein band intensity normalized to GAPDH, expressed as a relative fold change to the gene free control (n = 9). A two-tailed mean value T test determined significance (**$p < 0.01$) (– Donor 1, – Donor 2, –Donor 3).

Gene Activated Scaffolds Upregulated SOX9 mRNA Expression at Day 7

Reinforced scaffolds were gene activated with SOX9 NPs to assess their effect on chondrogenic differentiation of hMSCs in culture. After seven days in culture, qRT-PCR was utilized to compare gene expression of *SOX9*, *COL2a1*, and *ACAN* between cells on SOX9 activated and gene free scaffolds (Fig. 2). Individually all three hMSC donor populations had significant increases in the SOX9 mRNA (n = 3, p = 0.0248, p = 0.0467, p = 0.0007 respectively) expression after 7 days, when cultured on SOX9 activated scaffolds in comparison to gene free controls. Although, when the 3 datasets were merged, the total variance between the 3 donor groups meant that a statistically significant increase in *SOX9* mRNA was not observed (p = 0.0631). Upregulation of *COL2α1* mRNA on SOX9 activated scaffolds was significant (n = 9, p = 0.017), whereas the increase in *ACAN* expression was not significantly different (n = 9, p = 0.1080) from the gene free control.

Gene Activated Scaffolds Led to Elevated SOX9 Protein Expression in hMSCs

Seven days after hMSCs were seeded on the SOX9 activated scaffolds or gene free control, SOX9 protein expression was assessed by western blot. Cells on the SOX9 activated scaffolds had greater expression of SOX9 compared to cells on the gene free control (Fig. 3**a**). This was confirmed by quantifying the relative intensity of SOX9 protein band normalized to their GAPDH protein expression (Fig. 3**b**).

hMSCs Cultured on SOX9 Activated Scaffolds Upregulated Pro-Chondrogenic Genes

After 28 days in culture the ability of SOX9 activated scaffolds to induce hMSC chondrogenic differentiation was quantifiably evident. qRT-PCR indicated that both SOX9 NPs and LPN were effective at raising *SOX9* mRNA expression by two orders of magnitude over the gene free control (Fig. 4**a**). While the increase was insignificant, this is likely caused by the variance (σ) in how individual donor populations responded to the treatment conditions (σ, gene free = 0.429, SOX9 activated = 151,379, LNP = 476,189). When looking at downstream pro-chondrogenic targets that SOX9 directly regulates, such as type II collagen (*COL2α1*) (Fig. 4**b**) or aggrecan (*ACAN*) (Fig. 4**c**), both genes were significantly upregulated on the SOX9 activated scaffold compared to gene free control, even with donor variation (σ = 3262.91). In contrast, the LNP control showed no increase in mRNA expression of downstream SOX9 targets (*COL2α1*, *ACAN*), which was a somewhat surprising finding since both SOX9 NP activated and LNP seemed to have similar success in upregulating *SOX9* mRNA.

Expression of the other SOX-trio pro-chondrogenic transcriptional factors *SOX5* (Fig. 4**d**) and *SOX6* (Fig. 4**e**)

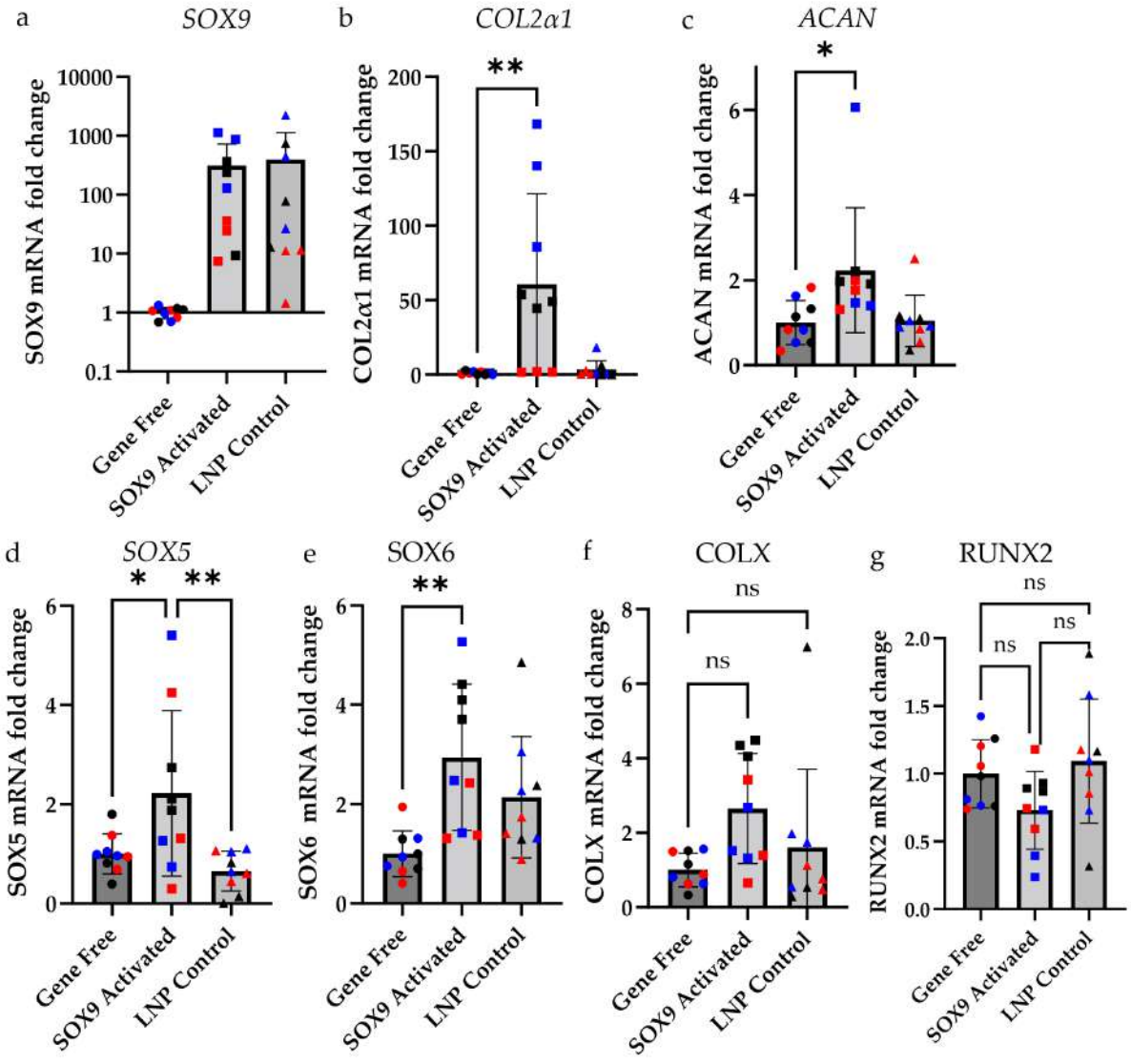

Fig. 4. hMSCs cultured on SOX9 activated scaffolds significantly increased pro-chondrogenic genes, without activating hypertrophic genes. qRT-PCR of hMSCs after 28 days on gene free, SOX9 activated, and LNP controls. Relative mRNA expression of: *SOX9* (**a**), *COL2α1* (**b**), *ACAN* (**c**), *SOX5* (**d**), *SOX6* (**e**), *COLX* (**f**), and *RUNX2* (**g**). A one-way ANOVA with Tukey post-test determined significance, ($n = 9$, $^{*}p < 0.05$, $^{**}p < 0.01$, ns = non-significant) (– Donor 1, – Donor 2, –Donor 3).

was also analyzed. Only hMSCs cultured on SOX9 activated scaffolds demonstrated a significant increase in both *SOX5* and *SOX6* mRNA. Expression levels of hypertrophic genes COLX (Fig. 4**f**), and RUNX2 (Fig. 4**g**) were then analyzed. While there was a slight increase in the mean expression of COLX from hMSCs on the SOX9 activated compared to the gene free control, the increase was not significant ($p > 0.05$). Similarly, hMSC on SOX9 activated scaffolds showed no significant increase in RUNX2 versus the gene free control. Interestingly, though not statistically significant ($p = 0.2407$), hMSC on SOX9 activated scaffolds had a 27 % reduction in mean RUNX2 mRNA expression compared to the gene free control.

SOX9 upregulation enhanced COL2 protein production

Along with qRT-PCR, western blot analysis 28 days after hMSCs were seeded on SOX9 activated, gene free, or LNP controls confirmed that SOX9 NP activation resulted in physiologically relevant increase of essential hyaline cartilage ECM protein COL2 (Kannu *et al*., 2012). hMSCs from all 3 donors exhibited a significant increase in COL2 protein deposition on SOX9 activated scaffolds when compared with their gene free control (Fig. 5**a**,**b**). Interestingly, hMSC from one donor (Donor 1) on the LNP scaffold produced a significant increase in COL2 over its gene free control ($n = 3$, $p = 0.0425$). However, this trend was not observed with hMSC from the other 2 donors, with no significant change in COL2 expression in LNP samples observed

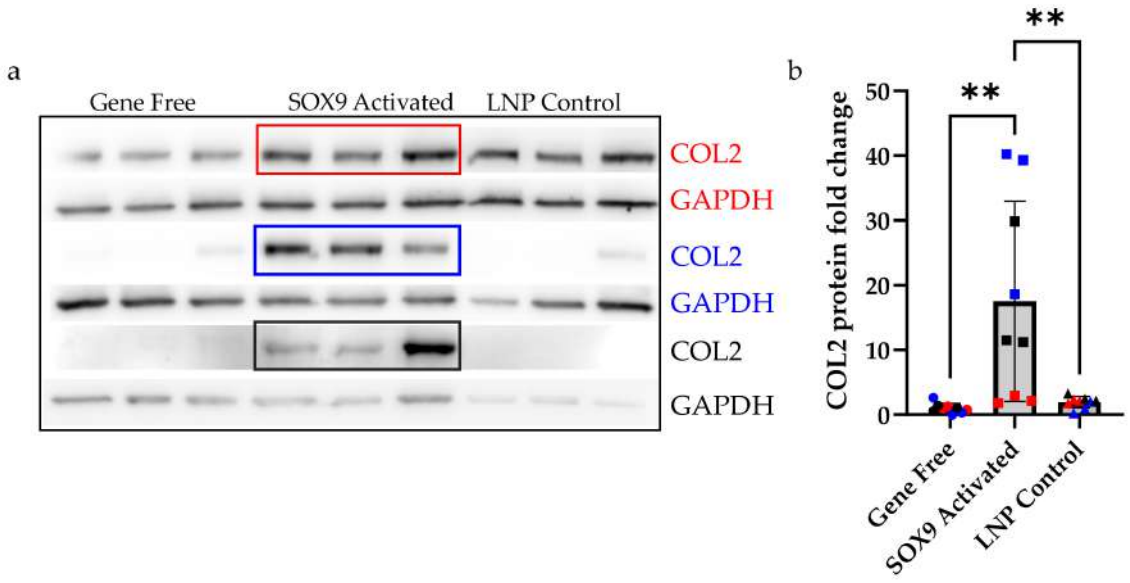

Fig. 5. Structural ECM protein COL2 was significantly upregulated in hMSCs cultured on SOX9 activated scaffolds after 28 days. (**a**) COL2, and GAPDH protein expression from cells on gene free, SOX9 activated and LNP controls. (**b**) Quantified protein band intensity expressed as a relative fold change per donor specific gene free control ($n = 9$). A one-way ANOVA with Tukey post-test determined significance, ($n = 9$, $^{**}p < 0.01$) ─ Donor 1, ─ Donor 2, ─Donor 3.

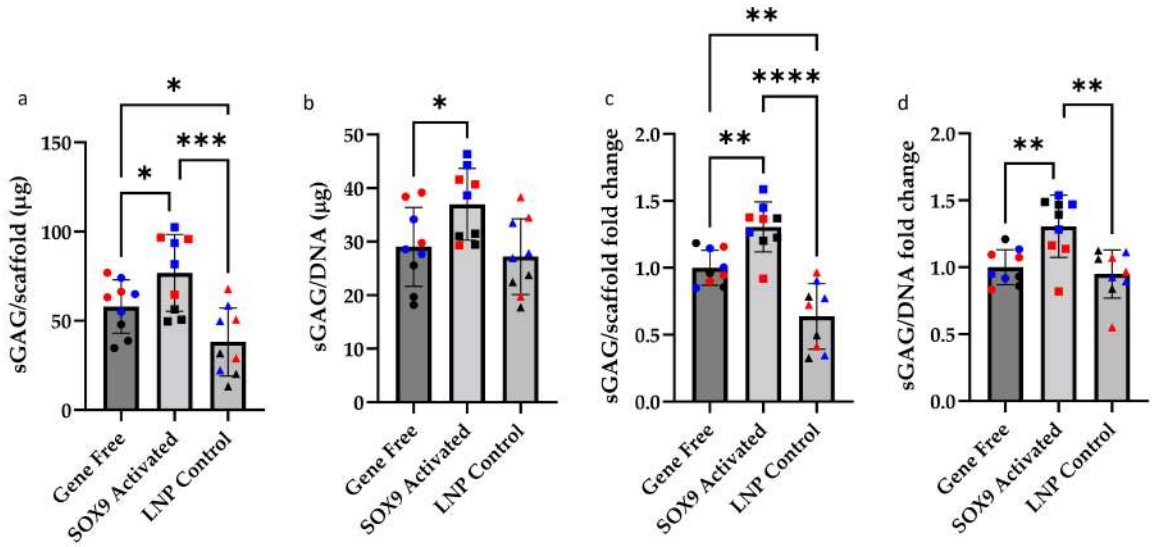

Fig. 6. sGAG production was significantly upregulated from hMSC cultured in SOX9 activated scaffolds after 28 days *in vitro*. (**a**) sGAG/Scaffold from hMSC on gene free, SOX9 activated and LNP controls. (**b**) Total sGAG normalized to DNA content per scaffold. (**c**) Relative fold change of total sGAG normalized to individual donor gene free control mean sGAG. Relative fold change of (sGAG/DNA) normalized to individual donor gene free mean (**d**). (**a,b**) were analyzed using one-way ANOVA with Fisher's LSD test ($n = 9$, $^{*}p < 0.05$, $^{***}p < 0.001$). (**c,d**) were analyzed with a one-way ANOVA with a Tukey post-hoc test ($n = 9$, $^{*}p < 0.05$, $^{**}p < 0.01$, $^{***}p < 0.001$, $^{****}p < 0.0001$) ─ Donor 1, ─ Donor 2, ─Donor 3.

when aggregating the data from the 3 donors ($n = 9$, $p = 0.97$).

SOX9 Activation Enhanced Hyaline Matrix Deposition by hMSC on Reinforced Scaffolds

After 28 days *in vitro*, sGAG deposited from hMSC seeded on SOX9 activated scaffolds, LNP and gene free controls was quantified to assess chondrogenic differentiation. hMSCs on the SOX9 activated scaffold produced a significantly greater quantity of sGAG compared with the gene free control ($p = 0.0427$) (Fig. 6**a**), and LNP control ($p = 0.0002$). When normalized to DNA content per scaffold, the SOX9 NPs treatment maintained a significant increase in sGAG/DNA ($p = 0.0453$) over the gene free con-

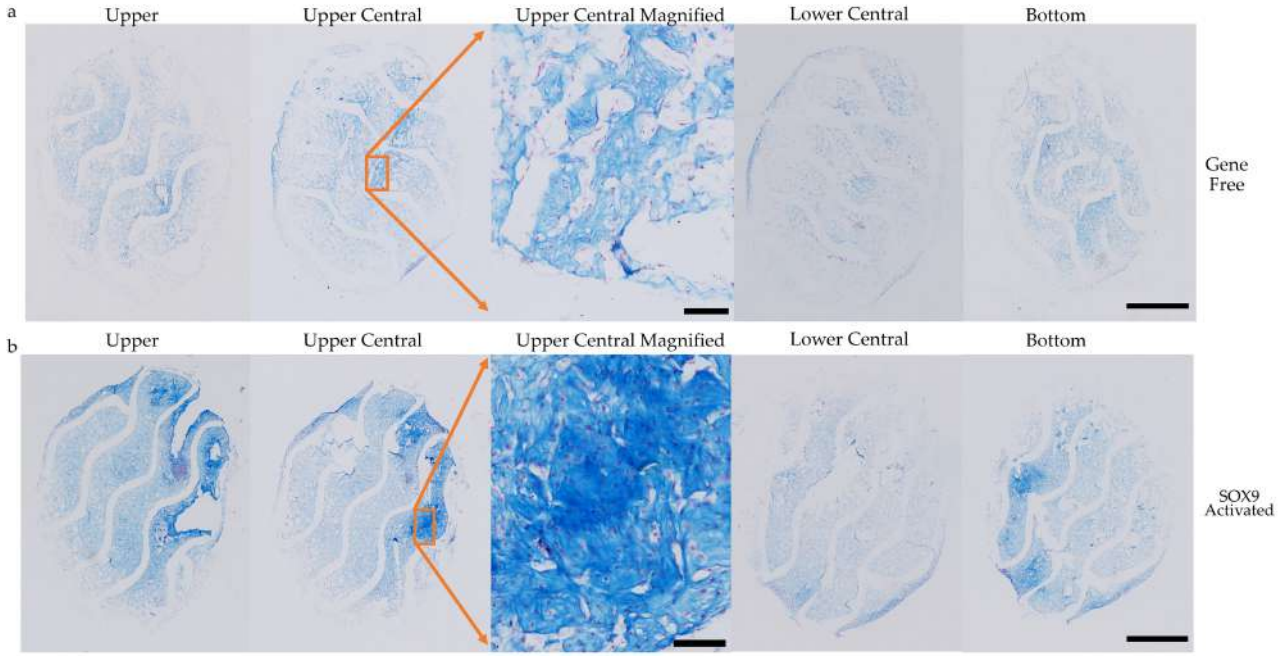

Fig. 7. Greater sGAG deposition was observed from hMSCs cultured on the SOX9 activated scaffolds compared to gene free control. Representative cross-section images from upper, upper-central, magnified upper-central (scale = 200 µm), lower-central, and bottom regions of the gene free control (**a**), and SOX9 activated scaffold (**b**) stained with Alcian Blue (pH1), and counterstained with nuclear fast red. Scale bar = 3000 µm.

trol (Fig. 6**b**). To reduce variance stemming from different basal levels of sGAG production amongst donor groups. Total sGAG, and sGAG/DNA were further normalized as a fold change of mean sGAG per donor specific gene free control scaffolds to better elucidate how treatment conditions were affecting cellular sGAG production. Under these conditions, there was a significant increase in the relative sGAG/scaffold production by cells in the SOX9 activated scaffolds compared with the gene free control ($p = 0.007$) (Fig. 6**c**). The LNP control produced significantly less sGAG compared to the gene free control ($p = 0.0015$). Similarly, there was a significant increase in donor normalized sGAG/DNA from cells on the SOX9 activated scaffolds compared with the gene free control ($p = 0.0051$), or LNP control ($p = 0.0012$) (Fig. 6**d**).

Improved Distribution of sGAG on Gene Activated Scaffolds

After 28 days culture, histological assessment of the distribution of sGAG produced by hMSCs cultured on the SOX9 activated scaffold confirmed production of an ECM more indicative of healthy hyaline cartilage when compared to gene free control. Serial cross-sections with 4 representative images from the upper (1500-2000 µm), upper central (1000-1500 µm), lower central (500-1000 µm), and bottom (0-500 µm) regions of the scaffolds show greater sGAG distribution throughout all stratifications of the reinforced SOX9 activated scaffolds (Fig. 7**a**). A magnified analysis of the upper-central region indicated higher cell density on SOX9 activated scaffold, with more circular nuclei and larger cell volume, which is more indicative of a chondrocyte morphology, compared to the gene free control (Fig. 7**b**).

COL2 Protein Deposition and Distribution was Improved in Gene Activated Scaffolds

Immunohistochemistry confirmed and corroborated qRT-PCR and WB data indicating greater COL2 protein deposition in SOX9 activated scaffolds. Representative whole slice layers (10 µm thick) were imaged from all three donor groups (Fig. 8**a**,**b**). IHC staining indicated enhanced COL2 deposition in SOX9 activated scaffolds when compared with respective gene free controls. With magnified regions of interest (Fig. 8**c**,**d**) indicating that COL2 deposition in SOX9 activated scaffolds occupied the void space within the existing scaffold microporous architecture, whereas COL2 deposition on control scaffolds appeared confined to the surface of the microporous architecture. These findings are well aligned with the qRT-PCR and WB findings and further provide evidence that gene activation of a pro-chondrogenic mechanically reinforced PCL-CHyA scaffolds with SOX9 NPs enhanced chondrogenic differentiation of hMSCs, which in turn enhanced the production of highly specialized ECM markers indicative of healthy hyaline tissue.

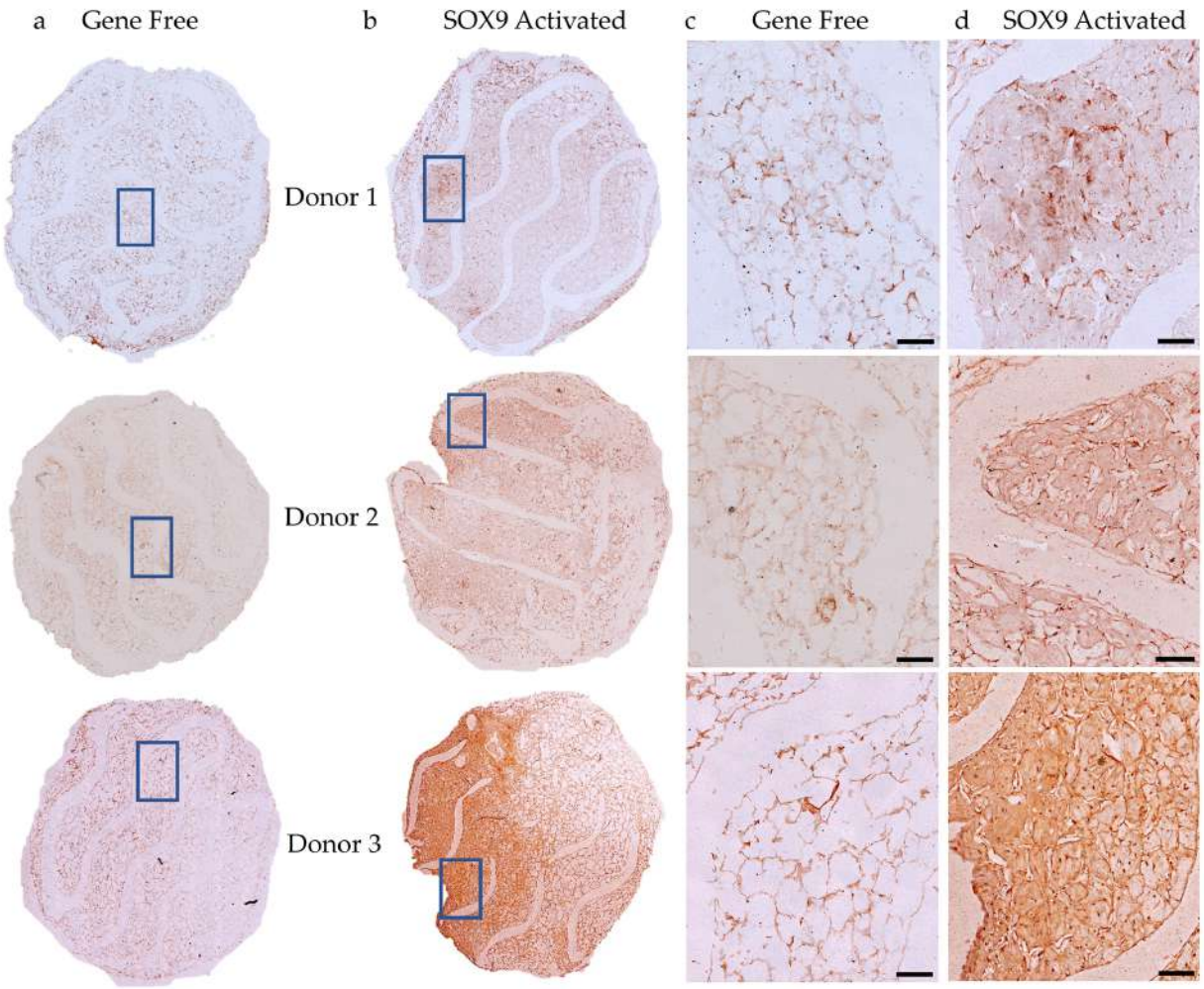

Fig. 8. Immunohistochemistry indicates greater COL2 deposition throughout SOX9 activated scaffolds. (**a**) Representative images of entire scaffold cross sections of gene free control and SOX9 activated scaffolds. (**b**) Magnified regions of interest (blue box) from each donor, gene free control (**c**) and SOX9 activated scaffolds (**d**). Scale bar = 200 µm. (abCOL2, Santa Cruz, 1:100).

Discussion

The objective of this study was to gene activate a mechanically reinforced biomaterial with a proven history of supporting chondrogenesis to further enhance production of hyaline-like ECM for the eventual treatment of large area AC defects including in tissues suffering from compromised biological functionality. The increasing prevalence of OA amongst younger populations, particularly following traumatic injury (post-traumatic OA) has motivated increased demand for innovative tissue engineering solutions to pre-emptively repair AC defects before the onset of OA (Pamilo *et al*., 2022; Inacio *et al*., 2017). To accomplish this goal, several challenges were addressed, including the engineering of a regenerative scaffold capable of both resisting the mechanical forces present in the joint and promoting the regeneration of articular-like cartilage through gene activation with SOX9 nanoparticles. We demonstrated that, following optimization of the GET NP and scaffold composition, that incorporating SOX9 NPs into the reinforced scaffold effectively transfected and promoted chondrogenic gene and protein expression in infiltrating hMSCs as they migrated into the scaffold. Their enhanced chondrogenic phenotype resulted in significantly enhanced production of specialized ECM components characteristic of articular cartilage, such as COL2 and sGAG, while not upregulating the expression of hypertrophic or fibrocartilage markers such as COLX and RUNX2. We propose this research has substantial impact as it expands the indication of use of a promising natural polymer-based pro-chondrogenic biomaterial to potentially allow effective treatment of large load bearing AC defects which are commonly seen clinically.

Delivery of SOX9 NPs incorporated into the reinforced scaffold was highly effective in this study and resulted in a > 300-fold upregulation of SOX9 mRNA expression in hMSCs when compared to the gene free control. Importantly for translation of this technology into human cartilage, a slowly healing tissue, this expression remained elevated even after 28 days in culture. Upregulation

of *SOX9* also resulted in significant upregulation of downstream transcriptional targets *COL2α1* and *ACAN*, along with other pro-chondrogenic transcription factors *SOX5* and *SOX6* after 28 days. Both western blot analysis and immunohistological staining indicated superior COL2 protein expression compared to the gene free scaffolds. Similarly greater sGAG production on SOX9 activated scaffolds was quantified and corroborated with Alcian Blue staining. These downstream effects following SOX9 upregulation are significant as they are central to the success of this approach but also are not always observed in previous studies involving upregulation of SOX9 (Carballo-Pedrares *et al*., 2022; Kupcsik *et al*., 2010; Kim *et al*., 2011). Indeed, in this study, LNP controls were observed to increase SOX9 mRNA expression in hMSCs to similar levels observed with GET NPs but failed to demonstrate any benefit on downstream upregulation of chondrogenic SOX9 targets like *COL2α1*, and *ACAN*. Similarly, Carballo-Pedrares *et al.* (2022) reported a less than 2 fold increase in *COL2α1* mRNA after lipofectamine-mediated delivery of SOX9 to hMSCs. Here, hMSCs on the SOX9 activated scaffolds with GET NPs had normal metabolic activity relative to gene free controls, while LNP delivery had a negative impact on the metabolic activity of hMSCs, which likely resulted in decreased chondrogenic gene expression downstream of SOX9 (Fig. 1**c**-**e**). Taken together, these results indicate the non-trivial nature of the gene activated reinforced scaffold platform design developed here and the strong potential for the developed SOX9 activated scaffold system for future *in vivo* translation and utility in repair of large area load bearing chondral defects.

A strength of this study was the design and synergistic integration of mechanically reinforced biomaterials, with pro-chondrogenic gene delivery technologies to create an off-the-shelf gene-activated, reinforced regenerative biomaterial. While previous studies have individually documented the advantage of mechanical reinforcement or gene therapies on cartilage regeneration (Matsiko *et al*., 2012; Intini *et al*., 2022; Raftery *et al*., 2020; Matsiko *et al*., 2015), to the best of our knowledge there are no published studies that complex reinforced biomaterials with compressive moduli equivalent to healthy cartilage with gene therapies to further promote chondrogenesis (Yang *et al*., 2020). The promising *in vitro* results obtained here indicate the combination of mechanically reinforced SOX9 activated scaffolds with a common surgical microfracture technique to release bone marrow derived MSCs *in vivo* may improve the articular cartilage-like characteristics of regenerated tissue, enhancing a biomaterial approach that has shown excellent efficacy for focal defect repair (Levingstone *et al*., 2016; Raftery *et al*., 2019; Levingstone *et al*., 2016).

The results described in this study were obtained in static and normoxic culture conditions, which have previously been reported to be suboptimal for chondrogenic differentiation of hMSCs (Grodzinsky *et al*., 2000; Anderson & Johnstone, 2017). We note that previous studies involving pSOX9 delivery have indicated expression of SOX9 transgene also requires mechanically-loaded culture conditions to produce significant increases in sGAG secretion by hMSCs (Kupcsik *et al*., 2010). In this study, the synergistic effect of our gene delivery system and reinforced regenerative scaffold was sufficient to significantly increase sGAG production, without the need for additional mechanical loading. Furthermore, it is likely that the presence of the reinforced framework in SOX9 activated scaffolds, which increased the compressive modulus to mimic the native range of healthy AC, will enhance cell responses further in an *in vivo* setting by allowing loading and thus enhancing the mechanoresponsiveness of the cells while shielding them from harmful injurious stresses that might have occurred in a non-reinforced scaffold. The intrinsic properties of the SOX9 activated scaffold resulting from reinforcement could thus impact cell-level anabolic responses within scaffolds through local alterations in ECM stiffness sensing and mechano-transductive signaling (Hodgkinson *et al*., 2022). Though not investigated directly, the results presented here demonstrating increased sGAG, are in agreement with our previous work comparing sGAG production in reinforced and non-reinforced regenerative scaffolds (Selig *et al*., 2020; Hall, 2019).

Localization and longevity of gene delivery to articular cartilage remains a challenge for effective regeneration. The non-viral SOX9 activated scaffold developed here resulted in a 100× upregulation in mean *SOX9* mRNA expression at 7 days, which was sustained for at least 28 days. Similarly, our results show a significant 5-fold increase in COL2 mRNA expression at day 7 (Fig. 2) which develops to a 60-fold (Fig. 4**b**) increase at day 28. This system compares favourably to alternative approaches involving functionalization of biomaterials for viral gene delivery (Venkatesan *et al*., 2020), resulting in greater transgene and downstream chondrogenic gene expression, while providing safety and ease-of-production benefits. These *in vitro* results provide promising evidence that this approach can locally deliver physiologically relevant concentrations of SOX9 to bone marrow derived MSCs invading SOX9 activated scaffolds *in vivo*. In support of this, a pro-chondrogenic biomaterial previously developed by our laboratory, which was functionalized for simultaneous delivery of plasmids for the SOX-Trio factors (pSOX5, pSOX6, pSOX9) resulted in excellent chondrogenic responses that were comparable *in vitro* and *in vivo* (Raftery *et al*., 2020). The results presented in the current paper delivering a single SOX9 plasmid on a mechanically reinforced scaffold produced comparable results *in vitro* to those reported when previously delivering three chondrogenic plasmids, streamlining this previously successful approach. Additionally, this method could be adapted to knock down or silence gene expression of anti-chondrogenic and pro-inflammatory pathways by delivering micro-RNA (miR) or

small interfering RNA (siRNA) in addition to upregulating SOX9 (Castaño *et al*., 2023). Furthermore, reinforcement increases the utility of the gene activated scaffold for applications involving load bearing cartilage regions and large defects where biomaterials are prone to delamination from defect sites. Moreover, these findings suggest the PCL reinforcing framework did not interfere with GET NPs ability to effectively transfect infiltrating hMSC compared with non-reinforced CHyA matrices (Joyce *et al*., 2023; Raftery *et al*., 2020). With no effective surgical interventions currently available other than total joint replacement surgeries, which are considered a terminal treatment option, mechanically reinforced SOX9 activated scaffolds could fulfill the niche demand for an intermediate surgical intervention to treat large area AC defects. This would potentially increase the quality of life for patients, and potentially mitigating the progression of OA, and its ever-increasing burden on global healthcare systems.

Taken together, these gene activated mechanically reinforced scaffolds show potential as an off-the-shelf biomaterial to repair large area, load bearing chondral defects. Though an *in vivo* study is required to further validate its potential for successful clinical translation, these findings are promising. Additionally, peripheral areas of research may also benefit from this study, as the techniques utilized here could be tailored for other tissue specific applications. For example, dental or bone tissue engineering applications could benefit from the stiffer reinforcing scaffold described here, while gene activation of periodontal, or osteogenic genes with similar techniques as described here might further enhance healing (Li *et al*., 2022; Tsutsui, 2020; Cunniffe *et al*., 2017). While the SOX9 activated scaffold was specifically designed to treat load bearing articular cartilage defects, similar biomaterials could thus be biofabricated to regenerate many different types of tissue.

Conclusion

This study successfully gene activated a mechanically reinforced biomimetic scaffold with a master chondrogenic regulator leading to an enhanced ECM production indicative of healthy articular cartilage. Targeted upregulation of SOX9 was sufficient to promote expression of *SOX5* & *SOX6* transcription factors—known together as the SOX-Trio chondrogenic factors. Downstream transcriptional targets of SOX9 (COL2, ACAN) were also upregulated leading to higher quality ECM production, more closely representing healthy hyaline cartilage while hypertrophic genes; COLX and RUNX2 were not significantly upregulated. Therefore, gene activation with the GET system to deliver DNA in reinforced biomimetic scaffolds could offer an off-the-shelf solution to repair large, load bearing articular cartilage defects. This novel biomaterial has immense clinical translation potential, offering orthopedic surgeons a new tool to regenerate damaged cartilage tissue rather than replacing it.

List of Abbreviations

AC, Articular cartilage; OA, osteoarthritis; ECM, extra cellular matrix; PCL, polycaprolactone; CHyA, collagen hyaluronic acid; GA, gene-activated; NPs, nanoparticles; GET, glycosaminoglycan-binding enhanced transduction; hMSC, human mesenchymal stromal cells; sGAG, sulphated glycosaminoglycans; US, United States; rGFs, recombinant growth factors; EDAC, 1-Ethyl-3-(3(dimethlaminopropyl)-carbodimide; NHS, N-Hydroxysuccinimide; CR, charge ratios; CCM, Complete chondrogenic media; GM, growth media; DMEM, Dulbecco's Modified Eagle Medium; ICC, Immunocytochemistry; WB, Western blot; IHC, immunohistochemical; ANOVA, analysis of variance; CI, confidence interval.

Availability of Data and Materials

The data used to support the findings of this study are available from the corresponding author upon request.

Author Contributions

M.J. was responsible for methodology, experimental design, biofabrication, biological evaluation, interpretation and processing of data, and manuscript revisions. T.H. contributed to methodology, biological evaluation, and manuscript revision. C.I. was responsible for methodology, biofabrication, biological evaluations and manuscript revisions. J.E.D was responsible for conception of design, creation of GET, methodologies, and manuscript revision. D.J.K. was responsible for conceptualization and manuscript revision. F.J.O. contributed to conceptualisation, funding acquisition, experimental design, methodology and manuscript revision.

Ethics Approval and Consent to Participate

Not applicable.

Acknowledgments

This study has received funding from the European Research Council under the European Community's Horizon 2020 research and innovation programme under ERC Advanced Grant agreement n° 788753 (ReCaP). TH benefits from funding support from Science Foundation Ireland (SFI) under Grant number: 21/PATH-S/9306.

Funding

This research received no external funding.

Conflict of Interest

The authors declare no conflict of interest. FJO is serving the Editorial Board members of this journal. We declare that FJO had no involvement in the peer review of this article and has no access to information regarding its peer review. Full responsibility for the editorial process for this article was delegated to CC.

References

Abu Awwad HADM, Thiagarajan L, Kanczler JM, Amer MH, Bruce G, Lanham S, Rumney RMH, Oreffo ROC, Dixon JE (2020) Genetically-programmed, mesenchymal stromal cell-laden & mechanically strong 3D bioprinted scaffolds for bone repair. Journal of Controlled Release: Official Journal of the Controlled Release Society 325: 335-346. DOI: 10.1016/j.jconrel.2020.06.035.

Anderson DE, Johnstone B (2017) Dynamic Mechanical Compression of Chondrocytes for Tissue Engineering: A Critical Review. Frontiers in Bioengineering and Biotechnology 5: 76. DOI: 10.3389/fbioe.2017.00076.

Aytekin K, Esenyel CZ (2021) Comparing BST-CarGel® with Hyalofast for the Treatment of Hyaline Cartilage Defects. European Archives of Medical Research 37: 217–222. DOI: 10.4274/eamr.galenos.2020.76983.

Billings E, Jr, von Schroeder HP, Mai MT, Aratow M, Amiel D, Woo SL, Coutts RD (1990) Cartilage resurfacing of the rabbit knee. The use of an allogeneic demineralized bone matrix-autogeneic perichondrium composite implant. Acta Orthopaedica Scandinavica 61: 201-206. DOI: 10.3109/17453679008993501.

Blokpoel Ferreras LA, Chan SY, Vazquez Reina S, Dixon JE (2021) Rapidly Transducing and Spatially Localized Magnetofection Using Peptide-Mediated Non-Viral Gene Delivery Based on Iron Oxide Nanoparticles. ACS Applied Nano Materials 4: 167-181. DOI: 10.1021/acsanm.0c02465.

Blokpoel Ferreras LA, Scott D, Vazquez Reina S, Roach P, Torres TE, Goya GF, Shakesheff KM, Dixon JE (2020) Enhanced Cellular Transduction of Nanoparticles Resistant to Rapidly Forming Plasma Protein Coronas. Advanced Biosystems 4: e2000162. DOI: 10.1002/adbi.202000162.

Carballo-Pedrares N, Sanjurjo-Rodriguez C, Señarís J, Díaz-Prado S, Rey-Rico A (2022) Chondrogenic Differentiation of Human Mesenchymal Stem Cells via SOX9 Delivery in Cationic Niosomes. Pharmaceutics 14: 2327. DOI: 10.3390/pharmaceutics14112327.

Castaño IM, Raftery RM, Chen G, Cavanagh B, Quinn B, Duffy GP, Curtin CM, O'Brien FJ (2023) Dual scaffold delivery of miR-210 mimic and miR-16 inhibitor enhances angiogenesis and osteogenesis to accelerate bone healing. Acta Biomaterialia 172: 480-493. DOI: 10.1016/j.actbio.2023.09.049.

Chen L, Liu J, Guan M, Zhou T, Duan X, Xiang Z (2020) Growth Factor and Its Polymer Scaffold-Based Delivery System for Cartilage Tissue Engineering. International Journal of Nanomedicine 15: 6097-6111. DOI: 10.2147/IJN.S249829.

Cohen NP, Foster RJ, Mow VC (1998) Composition and dynamics of articular cartilage: structure, function, and maintaining healthy state. The Journal of Orthopaedic and Sports Physical Therapy 28: 203-215. DOI: 10.2519/jospt.1998.28.4.203.

Critchley S, Sheehy EJ, Cunniffe G, Diaz-Payno P, Carroll SF, Jeon O, Alsberg E, Brama PAJ, Kelly DJ (2020) 3D printing of fibre-reinforced cartilaginous templates for the regeneration of osteochondral defects. Acta Biomaterialia 113: 130-143. DOI: 10.1016/j.actbio.2020.05.040.

Cunniffe GM, Gonzalez-Fernandez T, Daly A, Sathy BN, Jeon O, Alsberg E, Kelly DJ (2017) * Three-Dimensional Bioprinting of Polycaprolactone Reinforced Gene Activated Bioinks for Bone Tissue Engineering. Tissue Engineering. Part a 23: 891-900. DOI: 10.1089/ten.tea.2016.0498.

Deirmengian CA, Lonner JH (2008) What's new in adult reconstructive knee surgery. The Journal of Bone and Joint Surgery. American Volume 90: 2556-2565. DOI: 10.2106/JBJS.H.01106.

Eltaher HM, Blokpoel Ferreras LA, Jalal AR, Dixon JE (2022) Direct contact-mediated non-viral gene therapy using thermo-sensitive hydrogel-coated dressings. Biomaterials Advances 143: 213177. DOI: 10.1016/j.bioadv.2022.213177.

Grodzinsky AJ, Levenston ME, Jin M, Frank EH (2000) Cartilage tissue remodeling in response to mechanical forces. Annual Review of Biomedical Engineering 2: 691-713. DOI: 10.1146/annurev.bioeng.2.1.691.

Hall AC (2019) The Role of Chondrocyte Morphology and Volume in Controlling Phenotype-Implications for Osteoarthritis, Cartilage Repair, and Cartilage Engineering. Current Rheumatology Reports 21: 38. DOI: 10.1007/s11926-019-0837-6.

Haudenschild DR, Chen J, Pang N, Lotz MK, D'Lima DD (2010) Rho kinase-dependent activation of SOX9 in chondrocytes. Arthritis and Rheumatism 62: 191-200. DOI: 10.1002/art.25051.

Haugh MG, Murphy CM, McKiernan RC, Altenbuchner C, O'Brien FJ (2011) Crosslinking and mechanical properties significantly influence cell attachment, proliferation, and migration within collagen glycosaminoglycan scaffolds. Tissue Engineering. Part a 17: 1201-1208. DOI: 10.1089/ten.TEA.2010.0590.

Hodgkinson T, Amado IN, O'Brien FJ, Kennedy OD (2022) The role of mechanobiology in bone and cartilage model systems in characterizing initiation and progression of osteoarthritis. APL Bioengineering 6: 011501. DOI: 10.1063/5.0068277.

Hodgkinson T, Kelly DC, Curtin CM, O'Brien FJ (2022) Mechanosignalling in cartilage: an emerging target for the treatment of osteoarthritis. Nature Reviews. Rheumatology 18: 67-84. DOI: 10.1038/s41584-021-00724-w.

Holland TA, Tabata Y, Mikos AG (2005) Dual growth factor delivery from degradable oligo(poly(ethylene glycol) fumarate) hydrogel scaffolds for cartilage tissue engineering. Journal of Controlled Release: Official Journal of the Controlled Release Society 101: 111-125. DOI: 10.1016/j.jconrel.2004.07.004.

Hutmacher DW, Schantz T, Zein I, Ng KW, Teoh SH, Tan KC (2001) Mechanical properties and cell cultural response of polycaprolactone scaffolds designed and fabricated via fused deposition modeling. Journal of Biomedical Materials Research 55: 203-216. DOI: 10.1002/1097-4636(200105)55:2<203::aid-jbm1007>3.0.co;2-7.

Inacio MCS, Paxton EW, Graves SE, Namba RS, Nemes S (2017) Projected increase in total knee arthroplasty in the United States - an alternative projection model. Osteoarthritis and Cartilage 25: 1797-1803. DOI: 10.1016/j.joca.2017.07.022.

Intini C, Ferreras LB, Casey S, Dixon JE, Gleeson JP, O'Brien FJ (2023) An Innovative miR-Activated Scaffold for the Delivery of a miR-221 Inhibitor to Enhance Cartilage Defect Repair. Advanced Therapeutics 6: 2200329. DOI: 10.1002/adtp.202200329.

Intini C, Hodgkinson T, Casey SM, Gleeson JP, O'Brien FJ (2022) Highly Porous Type II Collagen-Containing Scaffolds for Enhanced Cartilage Repair with Reduced Hypertrophic Cartilage Formation. Bioengineering (Basel, Switzerland) 9: 232. DOI: 10.3390/bioengineering9060232.

Intini C, Lemoine M, Hodgkinson T, Casey S, Gleeson JP, O'Brien FJ (2022) A highly porous type II collagen containing scaffold for the treatment of cartilage defects enhances MSC chondrogenesis and early cartilaginous matrix deposition. Biomaterials Science 10: 970-983. DOI: 10.1039/d1bm01417j.

Jalal AR, Dixon JE (2020) Efficient Delivery of Transducing Polymer Nanoparticles for Gene-Mediated Induction of Osteogenesis for Bone Regeneration. Frontiers in Bioengineering and Biotechnology 8: 849. DOI: 10.3389/fbioe.2020.00849.

Jo A, Denduluri S, Zhang B, Wang Z, Yin L, Yan Z, Kang R, Shi LL, Mok J, Lee MJ, Haydon RC (2014) The versatile functions of Sox9 in development, stem cells, and human diseases. Genes & Diseases 1: 149-161. DOI: 10.1016/j.gendis.2014.09.004.

Joyce M, Hodgkinson T, Lemoine M, González-Vázquez A, Kelly DJ, O'Brien FJ (2023) Development of a 3D-printed bioabsorbable composite scaffold with mechanical properties suitable for treating large, load-bearingarticular cartilage defects. European Cells & Materials. 45: 158-172. DOI: 10.22203/eCM.v045a11.

Kabir W, Di Bella C, Choong PFM, O'Connell CD (2021) Assessment of Native Human Articular Cartilage: A Biomechanical Protocol. Cartilage 13: 427S-437S. DOI: 10.1177/1947603520973240.

Kannu P, Bateman J, Savarirayan R (2012) Clinical phenotypes associated with type II collagen mutations. Journal of Paediatrics and Child Health 48: E38-43. DOI: 10.1111/j.1440-1754.2010.01979.x.

Khaitov M, Nikonova A, Shilovskiy I, Kozhikhova K, Kofiadi I, Vishnyakova L, Nikolskii A, Gattinger P, Kovchina V, Barvinskaia E, Yumashev K, Smirnov V, Maerle A, Kozlov I, Shatilov A, Timofeeva A, Andreev S, Koloskova O, Kuznetsova N, Vasina D, Nikiforova M, Rybalkin S, Sergeev I, Trofimov D, Martynov A, Berzin I, Gushchin V, Kovalchuk A, Borisevich S, Valenta R, Khaitov R, Skvortsova V (2021) Silencing of SARS-CoV-2 with modified siRNA-peptide dendrimer formulation. Allergy 76: 2840–2854. DOI: 10.1111/all.14850.

Kim JH, Park JS, Yang HN, Woo DG, Jeon SY, Do HJ, Lim HY, Kim JM, Park KH (2011) The use of biodegradable PLGA nanoparticles to mediate SOX9 gene delivery in human mesenchymal stem cells (hMSCs) and induce chondrogenesis. Biomaterials 32: 268-278. DOI: 10.1016/j.biomaterials.2010.08.086.

Kupcsik L, Stoddart MJ, Li Z, Benneker LM, Alini M (2010) Improving chondrogenesis: potential and limitations of SOX9 gene transfer and mechanical stimulation for cartilage tissue engineering. Tissue Engineering. Part a 16: 1845-1855. DOI: 10.1089/ten.TEA.2009.0531.

Laiva AL, O'Brien FJ, Keogh MB (2021) Anti-Aging β-Klotho Gene-Activated Scaffold Promotes Rejuvenative Wound Healing Response in Human Adipose-Derived Stem Cells. Pharmaceuticals (Basel, Switzerland) 14: 1168. DOI: 10.3390/ph14111168.

Laiva AL, O'Brien FJ, Keogh MB (2021) SDF-1α Gene-Activated Collagen Scaffold Restores Pro-Angiogenic Wound Healing Features in Human Diabetic Adipose-Derived Stem Cells. Biomedicines 9: 160. DOI: 10.3390/biomedicines9020160.

Lee K, Silva EA, Mooney DJ (2011) Growth factor delivery-based tissue engineering: general approaches and a review of recent developments. Journal of the Royal Society, Interface 8: 153-170. DOI: 10.1098/rsif.2010.0223.

Lefebvre V, Angelozzi M, Haseeb A (2019) SOX9 in cartilage development and disease. Current Opinion in Cell Biology 61: 39-47. DOI: 10.1016/j.ceb.2019.07.008.

Leskinen J, Eskelinen A, Huhtala H, Paavolainen P, Remes V (2012) The incidence of knee arthroplasty for primary osteoarthritis grows rapidly among baby boomers: a population-based study in Finland. Arthritis and Rheumatism 64: 423-428. DOI: 10.1002/art.33367.

Levingstone TJ, Ramesh A, Brady RT, Brama PAJ, Kearney C, Gleeson JP, O'Brien FJ (2016) Cell-free multi-layered collagen-based scaffolds demonstrate layer specific regeneration of functional osteochondral tissue in caprine joints. Biomaterials 87: 69-81. DOI: 10.1016/j.biomaterials.2016.02.006.

Levingstone TJ, Thompson E, Matsiko A, Schepens A, Gleeson JP, O'Brien FJ (2016) Multi-layered collagen-based scaffolds for osteochondral defect repair in rabbits. Acta Biomaterialia 32: 149-160. DOI: 10.1016/j.actbio.2015.12.034.

Li CS, Zhang X, Péault B, Jiang J, Ting K, Soo C, Zhou YH (2016) Accelerated Chondrogenic Differentiation of Human Perivascular Stem Cells with NELL-1. Tissue Engineering. Part a 22: 272-285. DOI:

10.1089/ten.TEA.2015.0250.

Li Y, Duan X, Chen Y, Liu B, Chen G (2022) Dental stem cell-derived extracellular vesicles as promising therapeutic agents in the treatment of diseases. International Journal of Oral Science 14: 2. DOI: 10.1038/s41368-021-00152-2.

Long H, Liu Q, Yin H, Wang K, Diao N, Zhang Y, Lin J, Guo A (2022) Prevalence Trends of Site-Specific Osteoarthritis From 1990 to 2019: Findings from the Global Burden of Disease Study 2019. Arthritis & Rheumatology (Hoboken, N.J.) 74: 1172-1183. DOI: 10.1002/art.42089.

Lotz B, Bothe F, Deubel AK, Hesse E, Renz Y, Werner C, Schäfer S, Böck T, Groll J, von Rechenberg B, Richter W, Hagmann S (2021) Preclinical Testing of New Hydrogel Materials for Cartilage Repair: Overcoming Fixation Issues in a Large Animal Model. International Journal of Biomaterials 2021: 5583815. DOI: 10.1155/2021/5583815.

MacCraith E, Joyce M, do Amaral RJFC, O'Brien FJ, Davis NF (2022) Development and in vitro investigation of a biodegradable mesh for the treatment of stress urinary incontinence. International Urogynecology Journal 33: 2177-2184. DOI: 10.1007/s00192-022-05160-2.

Manual I. Internet Manual Downloaded from Blyscan Sulfated Glycosaminoglycan Assay General Protocol. Biocolor LTD. 2012. Available: https://assets-global.website-files.com/623c6aaf9b946bc877abcc61/64c2317b3dd3ad3ffee60a95_Blyscan-manual-webopt.pdf (Accessed: 31 August 2021).

Markides H, Newell KJ, Rudorf H, Ferreras LB, Dixon JE, Morris RH, Graves M, Kaggie J, Henson F, El Haj AJ (2019) Ex vivo MRI cell tracking of autologous mesenchymal stromal cells in an ovine osteochondral defect model. Stem Cell Research & Therapy 10: 25. DOI: 10.1186/s13287-018-1123-7.

Matsiko A, Gleeson JP, O'Brien FJ (2015) Scaffold mean pore size influences mesenchymal stem cell chondrogenic differentiation and matrix deposition. Tissue Engineering. Part a 21: 486-497. DOI: 10.1089/ten.TEA.2013.0545.

Matsiko A, Levingstone TJ, Gleeson JP, O'Brien FJ (2015) Incorporation of TGF-beta 3 within collagen-hyaluronic acid scaffolds improves their chondrogenic potential. Advanced Healthcare Materials 4: 1175-1179. DOI: 10.1002/adhm.201500053.

Matsiko A, Levingstone TJ, O'Brien FJ, Gleeson JP (2012) Addition of hyaluronic acid improves cellular infiltration and promotes early-stage chondrogenesis in a collagen-based scaffold for cartilage tissue engineering. Journal of the Mechanical Behavior of Biomedical Materials 11: 41-52. DOI: 10.1016/j.jmbbm.2011.11.012.

Medvedeva EV, Grebenik EA, Gornostaeva SN, Telpuhov VI, Lychagin AV, Timashev PS, Chagin AS (2018) Repair of Damaged Articular Cartilage: Current Approaches and Future Directions. International Journal of Molecular Sciences 19: 2366. DOI: 10.3390/ijms19082366.

Mihalko WM, Haider H, Kurtz S, Marcolongo M, Urish K (2020) New materials for hip and knee joint replacement: What's hip and what's in kneed? Journal of Orthopaedic Research: Official Publication of the Orthopaedic Research Society 38: 1436-1444. DOI: 10.1002/jor.24750.

Niemeyer P, Angele P (2022) Autologous Chondrocyte Implantation (ACI) for Cartilage Defects of the Knee Using Novocart 3D and Novocart Inject. Operative Techniques in Sports Medicine 30: 150959. DOI: 10.1016/j.otsm.2022.150959.

Pamilo KJ, Haapakoski J, Sokka-Isler T, Remes V, Paloneva J (2022) Rapid rise in prevalence of knee replacements and decrease in revision burden over past 3 decades in Finland: a register-based analysis. Acta Orthopaedica 93: 382-389. DOI: 10.2340/17453674.2022.2266.

Park JS, Yang HN, Woo DG, Jeon SY, Do HJ, Lim HY, Kim JH, Park KH (2011) Chondrogenesis of human mesenchymal stem cells mediated by the combination of SOX trio SOX5, 6, and 9 genes complexed with PEI-modified PLGA nanoparticles. Biomaterials 32: 3679-3688. DOI: 10.1016/j.biomaterials.2011.01.063.

Power RN, Cavanagh BL, Dixon JE, Curtin CM, O'Brien FJ (2022) Development of a Gene-Activated Scaffold Incorporating Multifunctional Cell-Penetrating Peptides for pSDF-1α Delivery for Enhanced Angiogenesis in Tissue Engineering Applications. International Journal of Molecular Sciences 23: 1460. DOI: 10.3390/ijms23031460.

Qi H, Yang L, Li X, Sun X, Zhao J, Hou X, Li Z, Yuan X, Cui Z, Yang X (2019) Systemic administration of enzyme-responsive growth factor nanocapsules for promoting bone repair. Biomaterials Science 7: 1675-1685. DOI: 10.1039/c8bm01632a.

Raftery RM, Gonzalez Vazquez AG, Chen G, O'Brien FJ (2020) Activation of the SOX-5, SOX-6, and SOX-9 Trio of Transcription Factors Using a Gene-Activated Scaffold Stimulates Mesenchymal Stromal Cell Chondrogenesis and Inhibits Endochondral Ossification. Advanced Healthcare Materials 9: e1901827. DOI: 10.1002/adhm.201901827.

Raftery RM, Walsh DP, Blokpoel Ferreras L, Mencía Castaño I, Chen G, LeMoine M, Osman G, Shakesheff KM, Dixon JE, O'Brien FJ (2019) Highly versatile cell-penetrating peptide loaded scaffold for efficient and localised gene delivery to multiple cell types: From development to application in tissue engineering. Biomaterials 216: 119277 DOI: 10.1016/j.biomaterials.2019.119277.

Rao X, Huang X, Zhou Z, Lin X. An improvement of the 2ˆ(-delta delta CT) method for quantitative real-time polymerase chain reaction data analysis. Biostatistics, Bioinformatics and Biomathematics. 2013; 3: 71–85. Available at: https://www.ncbi.nlm.nih.gov/pmc/articles/PMC4280562/ (Accessed: 18 April 2021).

Rey-Rico A, Venkatesan JK, Schmitt G, Speicher-Mentges S, Madry H, Cucchiarini M (2018) Effective Remodelling of Human Osteoarthritic Cartilage by sox9 Gene Transfer and Overexpression upon Delivery of rAAV Vectors in Polymeric Micelles. Molecular Pharmaceutics 15: 2816-2826. DOI: 10.1021/acs.molpharmaceut.8b00331.

Ritchie A, Dixon JE, Clark P, Grabowska A (2020) The Jacket with Pulling Power a novel approach to early-stage evalulation of mangetic nanoparticles. Animal Technology and Welfare 19: 166-168. https://journal.atwjournal.com/atwaugust2020#page=1.

Rolfson O, Dahlberg LE, Nilsson JA, Malchau H, Garellick G (2009) Variables determining outcome in total hip replacement surgery. The Journal of Bone and Joint Surgery. British Volume 91: 157-161. DOI: 10.1302/0301-620X.91B2.20765.

Scheuing WJ, Reginato AM, Deeb M, Acer Kasman S (2023) The burden of osteoarthritis: Is it a rising problem? Best Practice & Research. Clinical Rheumatology 37: 101836. DOI: 10.1016/j.berh.2023.101836.

Schipani R, Scheurer S, Florentin R, Critchley SE, Kelly DJ (2020) Reinforcing interpenetrating network hydrogels with 3D printed polymer networks to engineer cartilage mimetic composites. Biofabrication 12: 035011. DOI: 10.1088/1758-5090/ab8708.

Selig M, Lauer JC, Hart ML, Rolauffs B (2020) Mechanotransduction and Stiffness-Sensing: Mechanisms and Opportunities to Control Multiple Molecular Aspects of Cell Phenotype as a Design Cornerstone of Cell-Instructive Biomaterials for Articular Cartilage Repair. International Journal of Molecular Sciences 21: 5399. DOI: 10.3390/ijms21155399.

Sheehy EJ, Kelly DJ, O'Brien FJ (2019) Biomaterial-based endochondral bone regeneration: a shift from traditional tissue engineering paradigms to developmentally inspired strategies. Materials Today. Bio 3: 100009. DOI: 10.1016/j.mtbio.2019.100009.

Sophia Fox AJ, Bedi A, Rodeo SA (2009) The basic science of articular cartilage: structure, composition, and function. Sports Health 1: 461-468. DOI: 10.1177/1941738109350438.

Thermo Fisher Scientific Inc. © LipofectamineTM 3000 Reagent Protocol Protocol. 2016. Available at: https://assets.thermofisher.com/TFS-Assets/LSG/manuals/lipofectamine3000_protocol.pdf (Accessed: 7 December 2022).

ThermoFisher. Quant-i(TM) PicoGreen (R) dsDNA Reagent and Kits. 2008; 1–7. Available at: https://www.thermofisher.com/document-connect/document-connect.html?url=https%3A%2F%2Fassets.thermofisher.com%2FTFS-Assets%2FLSG%2Fmanuals%2Fmp07581.pdf&title=UXVhbnQtaVQgUGljb0dyZWVuIGRzRE5BIFJlYWdlbnQgYW5kIEtpdHM= (Accessed: 16 March 2021).

Tsutsui TW (2020) Dental Pulp Stem Cells: Advances to Applications. Stem Cells and Cloning: Advances and Applications 13: 33-42. DOI: 10.2147/SCCAA.S166759.

Venkatesan JK, Gardner O, Rey-Rico A, Eglin D, Alini M, Stoddart MJ, Cucchiarini M, Madry H (2018) Improved Chondrogenic Differentiation of rAAV SOX9-Modified Human MSCs Seeded in Fibrin-Polyurethane Scaffolds in a Hydrodynamic Environment. International Journal of Molecular Sciences 19: 2635. DOI: 10.3390/ijms19092635.

Venkatesan JK, Meng W, Rey-Rico A, Schmitt G, Speicher-Mentges S, Falentin-Daudré C, Leroux A, Madry H, Migonney V, Cucchiarini M (2020) Enhanced Chondrogenic Differentiation Activities in Human Bone Marrow Aspirates via sox9 Overexpression Mediated by pNaSS-Grafted PCL Film-Guided rAAV Gene Transfer. Pharmaceutics 12: 280. DOI: 10.3390/pharmaceutics12030280.

Venkatesan JK, Schmitt G, Speicher-Mentges S, Orth P, Madry H, Cucchiarini M (2022) Effects of Recombinant Adeno-Associated Virus-Mediated Overexpression of Bone Morphogenetic Protein 3 on the Chondrogenic Fate of Human Bone Marrow-Derived Mesenchymal Stromal Cells. Human Gene Therapy 33: 950-958. DOI: 10.1089/hum.2022.004.

Visser J, Melchels FPW, Jeon JE, van Bussel EM, Kimpton LS, Byrne HM, Dhert WJA, Dalton PD, Hutmacher DW, Malda J (2015) Reinforcement of hydrogels using three-dimensionally printed microfibres. Nature Communications 6: 6933. DOI: 10.1038/ncomms7933.

Walsh DP, Raftery RM, Castaño IM, Murphy R, Cavanagh B, Heise A, O'Brien FJ, Cryan SA (2019) Transfection of autologous host cells in vivo using gene activated collagen scaffolds incorporating star-polypeptides. Journal of Controlled Release: Official Journal of the Controlled Release Society 304: 191-203. DOI: 10.1016/j.jconrel.2019.05.009.

Walsh DP, Raftery RM, Murphy R, Chen G, Heise A, O'Brien FJ, Cryan SA (2021) Gene activated scaffolds incorporating star-shaped polypeptide-pDNA nanomedicines accelerate bone tissue regeneration in vivo. Biomaterials Science 9: 4984-4999. DOI: 10.1039/d1bm00094b.

Yang R, Chen F, Guo J, Zhou D, Luan S (2020) Recent advances in polymeric biomaterials-based gene delivery for cartilage repair. Bioactive Materials 5: 990-1003. DOI: 10.1016/j.bioactmat.2020.06.004.

Zhao X, Shah D, Gandhi K, Wei W, Dwibedi N, Webster L, Sambamoorthi U (2019) Clinical, humanistic, and economic burden of osteoarthritis among noninstitutionalized adults in the United States. Osteoarthritis and Cartilage 27: 1618-1626. DOI: 10.1016/j.joca.2019.07.002.

Editor's note: The Scientific Editor responsible for this paper was Caroline Curtin.